

# NJC

Accepted Manuscript



This is an *Accepted Manuscript*, which has been through the Royal Society of Chemistry peer review process and has been accepted for publication.

*Accepted Manuscripts* are published online shortly after acceptance, before technical editing, formatting and proof reading. Using this free service, authors can make their results available to the community, in citable form, before we publish the edited article. We will replace this *Accepted Manuscript* with the edited and formatted *Advance Article* as soon as it is available.

You can find more information about *Accepted Manuscripts* in the [Information for Authors](#).

Please note that technical editing may introduce minor changes to the text and/or graphics, which may alter content. The journal's standard [Terms & Conditions](#) and the [Ethical guidelines](#) still apply. In no event shall the Royal Society of Chemistry be held responsible for any errors or omissions in this *Accepted Manuscript* or any consequences arising from the use of any information it contains.



Cite this: DOI: 10.1039/c0xx00000x

www.rsc.org/xxxxxx

ARTICLE TYPE

# Easily crosslinkable side-chain azobenzene polymers for fast and persistent fixation of surface relief gratings

Guang Han,<sup>a</sup> Hongtao Zhang,<sup>a</sup> Jing Chen,<sup>b</sup> Qian Sun,<sup>b</sup> Yuying Zhang<sup>a</sup> and Huiqi Zhang<sup>a\*</sup>*Received (in XXX, XXX) Xth XXXXXXXXX 20XX, Accepted Xth XXXXXXXXX 20XX*

DOI: 10.1039/b000000x

A series of side-chain azobenzene (azo) homo- and copolymers with easily crosslinkable N-hydroxysuccinimide carboxylate-substituted azo moieties and relatively low glass transition temperatures were synthesized for rapid and persistent fixation of surface relief gratings (SRGs). These azo polymers exhibited good thermal stability and their films proved easily crosslinkable within 4-15 min with 1,6-hexanediamine under mild conditions with the crosslinking rates of copolymer films being faster than homopolymer films. Moreover, the formation speed and saturation modulation depth of the photoinduced SRGs increased both with a decrease in the flexible spacer length in azo homopolymers and with an increase in the azo contents in copolymers. Furthermore, considerably stabilized high quality SRGs were obtained after their post-fixation by crosslinking, as revealed by the negligible or rather small change of both the modulation depth of the crosslinked SRGs upon their exposure to high temperatures or organic solvents and the transparency of the crosslinked polymer films.

## Introduction

Recent years have witnessed considerable interest in the azobenzene (azo)-containing polymers (azo polymers for short) due to their great potential in a wide range of applications such as nonlinear optical devices,<sup>1-3</sup> optical switching,<sup>4-7</sup> photo-controllable actuators,<sup>8-15</sup> holographic surface relief gratings (SRGs),<sup>16-30</sup> and so on. Among them, SRGs have attracted rapidly increasing attention because they are promising candidates for optical data storage,<sup>31, 32</sup> micro/nanopatterning<sup>28, 33-38</sup> and chemical sensing.<sup>39, 40</sup> SRGs can be inscribed on the azo polymer films at a temperature well below their glass transition temperatures ( $T_g$ ) upon irradiation with interfering polarization laser beams with an appropriate wavelength,<sup>41-44</sup> and they are erasable by thermal treatment or by irradiation with a uniform circularly polarized laser beam.<sup>20, 31, 45</sup> During this process, the azo molecules undergo a reversible trans-cis-trans isomerization and are aligned perpendicularly to the electrical field vector of the polarization light through the repetition of such isomerization cycles. Much evidence shows that the reversible surface modulations are caused by the photoinduced mass migration at the polymer film surfaces,<sup>46, 47</sup> and different models and theories have been proposed to elucidate the driving force.<sup>48-53</sup>

From a practical viewpoint, an important requirement for SRGs is their shape stability in terms of long-term storage and durability at higher temperatures. To address this issue, some research groups have adopted amorphous azo polymers with a high  $T_g$ ,<sup>54-57</sup> or liquid crystalline polymers with a high  $T_i$  (i.e., the liquid crystalline to isotropic phase transition temperature).<sup>58</sup> However, the SRGs formed on such azo polymers are not resistant to organic solvents, which significantly limits their

applications for patterning process.<sup>28, 34</sup> In addition, the fixation of the formed SRGs by their post-crosslinking have been proposed by the groups of Seki,<sup>59-61</sup> Rochon<sup>62</sup> and Kimura<sup>63</sup>, where crosslinkable side-chain azo polymers containing both non-crosslinkable azo groups and crosslinkable non-azo groups were used in all cases. The chemical crosslinking of such azo polymer films after their SRG inscription by using either a mixed vapor of hydrogen chloride and formaldehyde<sup>59, 60</sup> or ultraviolet (UV) irradiation<sup>61-63</sup> resulted in a drastic improvement of the shape stability of SRGs towards heat and solvent exposure. However, these two post-crosslinking methods have their inherent defects. The vapor-crosslinking strategy proved to not only take a rather long time (not less than 6 h),<sup>59, 60</sup> but also sometimes suffer from the damage of the SRG structure and lack of reproducibility.<sup>61</sup> Moreover, the use of hazardous formaldehyde should be avoided in view of health safety.<sup>61</sup> Although photo-crosslinking could be completed in 15 min, high-intensity UV irradiation may induce some photo-degradation of the azo chromophore and damage the SRG structure.<sup>62, 63</sup> Besides, some other approaches for obtaining stable SRGs also have the disadvantages of damaging the SRG structures or obviously decreasing the depth of the grating profile.<sup>64-66</sup>

Herein, we present a facile and highly efficient new post-crosslinking strategy for the fast and persistent fixation of the formed SRGs on the azo polymer films. A series of side-chain azo homopolymers and copolymers with incorporated N-hydroxysuccinimide carboxylate-substituted azo moieties were prepared for this purpose (Scheme 1). The N-hydroxysuccinimide carboxylate groups proved to be easily crosslinkable with a diamine, and the post-fixation procedure could be completed within 4-15 min under mild conditions (i.e., in a 1,6-



hexanediamine solution in methanol at ambient temperature) without obvious influence on the SRG structures. The fixed SRGs were stable at a temperature being about 10 °C above the  $T_g$  of the uncrosslinked azo polymers for at least 24 h or at 250 °C for 3 h with negligible or rather small reduction in their modulation depth, and the sinusoidal undulations also remained almost intact in the good organic solvent of the uncrosslinked azo polymers after 24 h. In addition, the incorporation of *n*-hexyl methacrylate (HMA) unit into the azo copolymers largely increased the crosslinking rate by improving the permeation of the crosslinker into the polymer films. *To our knowledge, this is the first report on the use of side-chain azo polymers with easily crosslinkable azo groups for the fixation of the photoinduced SRGs.* Such crosslinkable side-chain azo polymers have obvious advantages over the previously reported ones (which contained both the non-crosslinkable azo groups and crosslinkable non-azo groups<sup>59-63</sup>) because they could achieve much higher azo contents (e.g., a 100% azo content could be reached in case of azo homopolymers), which is highly useful for the more rapid and efficient formation of SRGs with large saturation modulation depth (as demonstrated in the following studies).

## Experimental section

### Materials

HMA (Tianjin Heowns Chemicals, China, 98%) was purified by passing through an alkaline alumina column before use. Tetrahydrofuran (THF, Tianjin Jiangtian Chemicals, China, 99%) was refluxed over sodium and then distilled. Azobisisobutyronitrile (AIBN, Tianjin Jiangtian Chemicals, chemical purity (CP)) was recrystallized from ethanol before use. Acryloyl chloride was prepared by the reaction between acrylic acid (Tianjin Damao Chemical Reagent Factory, China, 99.5%) and benzoyl chloride (Tianjin Jiangtian Chemicals, 98%). 4-((4-Hydroxy)phenylazo)benzoic acid, 4-((4- $\omega$ -hydroxyalkyloxy)phenylazo)benzoic acid (HAzoA-*m* (*m* = 2, 6, 10)), and 4-((4- $\omega$ -acryloyloxyalkyloxy)phenylazo)benzoic acid (AAzoA-*m* (*m* = 2, 6, 10)) were synthesized following our previous procedure (Scheme 1).<sup>67-69</sup> All the other reagents were commercially available and used without further purification unless otherwise stated.

### Synthesis of azo monomers

For convenience, the azo monomers with the *N*-hydroxysuccinimide carboxylate substituent (i.e., *N*-hydroxysuccinimide 4-((4- $\omega$ -acryloyloxyalkyloxy)phenylazo)benzoate) are named as M-*m*, where M refers to the monomer and *m* the number of the methylene unit in the flexible spacer. A series of azo monomers M-*m* (*m* = 2, 6, 10) were synthesized as shown below:

**Synthesis of M-10.** AAzoA-10 (3.00 g, 6.64 mmol) and *N*-hydroxysuccinimide (0.840 g, 7.30 mmol) were dissolved in dried THF (90 mL) and the solution was then cooled down to 0 °C. A solution of *N,N'*-dicyclohexylcarbodiimide (DCC) (1.367 g, 6.64 mmol) in dried THF (15 mL) was added dropwise into the above mixture with stirring. The obtained reaction solution was first stirred at 0 °C for 1 h and then at ambient temperature for 24 h. Finally, the reaction mixture was filtered and the filtrate was poured into a large amount of water (300 mL). The resulting

orange solid was purified by recrystallization in ethanol to provide the pure product (yield: 71%). Melting point (m.p.): 120-122 °C (determined by polarizing optical microscope (POM) at a heating rate of 10 °C/min). UV-vis (THF):  $\lambda_{\text{max}}/\text{nm}$  ( $\epsilon/\text{L mol}^{-1} \text{cm}^{-1}$ ) = 369 (26640), around 460 (not available due to the overlap of the absorption bands). <sup>1</sup>H NMR (300 MHz, CDCl<sub>3</sub>):  $\delta$  (ppm) = 8.28-8.21 (d, 2H, Ar-H), 8.00-7.85 (d, 4H, Ar-H), 7.04-6.95 (d, 2H, Ar-H), 6.43-6.32 (dd, 1H, CH<sub>2</sub>=C), 6.17-6.04 (dd, 1H, CH=C), 5.83-5.76 (dd, 1H, CH<sub>2</sub>=C), 4.19-4.10 (t, 2H, CH<sub>2</sub>O-), 4.09-4.00 (t, 2H, -OCH<sub>2</sub>), 2.94 (s, 4H, -COCH<sub>2</sub>CH<sub>2</sub>CO-), 1.88-1.23 (m, 16H, -(CH<sub>2</sub>)<sub>8</sub>-).

**Synthesis of M-2.** M-2 was prepared similarly as for M-10 (yield: 68%). m.p.: 146-148 °C (determined by POM at a heating rate of 10 °C/min). UV-vis (THF):  $\lambda_{\text{max}}/\text{nm}$  ( $\epsilon/\text{L mol}^{-1} \text{cm}^{-1}$ ) = 365 (25940), around 460 (not available due to the overlap of the absorption bands). <sup>1</sup>H NMR (300 MHz, CDCl<sub>3</sub>):  $\delta$  (ppm) = 8.30-8.21 (d, 2H, Ar-H), 8.01-7.90 (d, 4H, Ar-H), 7.10-7.00 (d, 2H, Ar-H), 6.51-6.42 (dd, 1H, CH<sub>2</sub>=C), 6.23-6.12 (dd, 1H, CH=C), 5.92-5.85 (dd, 1H, CH<sub>2</sub>=C), 4.60-4.52 (t, 2H, CH<sub>2</sub>O-), 4.36-4.28 (t, 2H, -OCH<sub>2</sub>), 2.94 (s, 4H, -COCH<sub>2</sub>CH<sub>2</sub>CO-).

**Synthesis of M-6.** M-6 was prepared similarly as for M-10 (yield: 75%). m.p.: 116-118 °C (determined by POM at a heating rate of 10 °C/min). UV-vis (THF):  $\lambda_{\text{max}}/\text{nm}$  ( $\epsilon/\text{L mol}^{-1} \text{cm}^{-1}$ ) = 369 (26760), around 460 (not available due to the overlap of the absorption bands). <sup>1</sup>H NMR (CDCl<sub>3</sub>):  $\delta$  (ppm) = 8.34-8.27 (d, 2H, Ar-H), 8.04-7.92 (d, 4H, Ar-H), 7.09-7.00 (d, 2H, Ar-H), 6.47-6.39 (dd, 1H, CH<sub>2</sub>=C), 6.20-6.10 (dd, 1H, CH=C), 5.88-5.81 (dd, 1H, CH<sub>2</sub>=C), 4.26-4.18 (t, 2H, CH<sub>2</sub>O-), 4.13-4.06 (t, 2H, -OCH<sub>2</sub>), 2.94 (s, 4H, -COCH<sub>2</sub>CH<sub>2</sub>CO-), 1.94-1.41 (m, 8H, -(CH<sub>2</sub>)<sub>4</sub>-).

### Synthesis of polymers

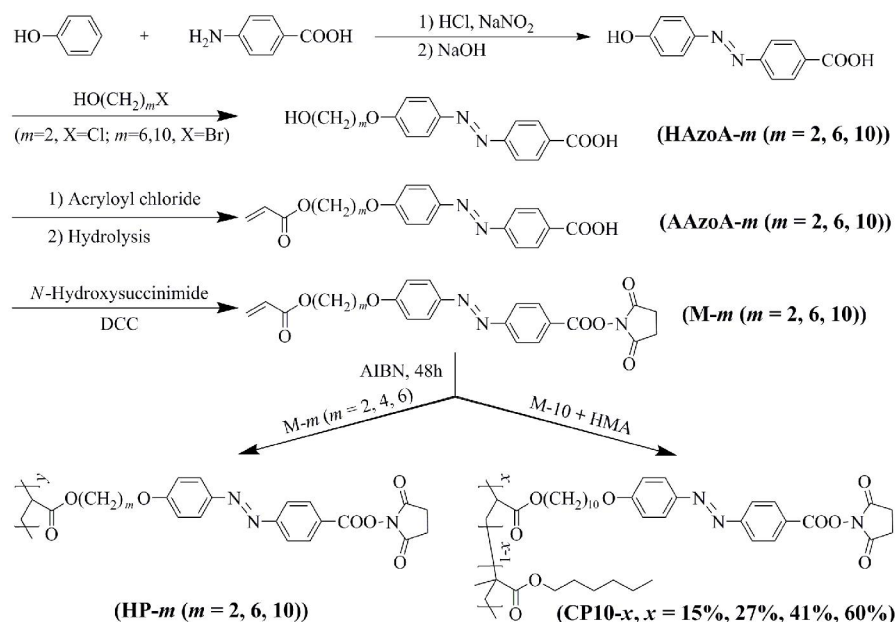
**Synthesis of side-chain azo homopolymers.** For convenience, the side-chain azo homopolymers with the *N*-hydroxysuccinimide carboxylate-substituted azo moieties are named as HP-*m*, where HP refers to the homopolymer and *m* the number of the methylene unit in the flexible spacer.

HP-*m* (*m* = 2, 6, 10) were prepared in anisole using AIBN as the initiator via the conventional free radical polymerization of M-*m*. A typical polymerization procedure for HP-10 is presented as follows: M-10 (400 mg, 0.73 mmol), AIBN (3.64 mg, 0.022 mmol) and freshly distilled anisole (6 mL) were added into a one-neck round-bottom flask (10 mL) and a clear solution was obtained after stirring. The reaction mixture was bubbled with argon for 20 min in an ice bath and the flask was then sealed and immersed into a thermostated oil bath at 70 °C and stirred for 48 h. After being cooled down to the room temperature, the polymerization mixture was added dropwise into methanol (80 mL) under stirring. The precipitate was collected by centrifugation and the obtained solid was washed thoroughly with warm methanol until no monomer was detectable with thin layer chromatography. Finally, the product was dried at 50 °C undervacuum for 48 h to provide the orange homopolymer HP-10 (yield: 35%, entry 3 in Table 1).

HP-2, HP-6, and the homopolymer of HMA (i.e., PHMA) were prepared following the similar process as for HP-10 (entries 1, 2, and 8 in Table 1).

**Synthesis of side-chain azo copolymers.** The copolymers of M-10 and HMA are named as CP10-*x*, where CP10 refers to the copolymer of M-10 and HMA and *x* the molar percentage of the





**Scheme 1** Synthetic route and chemical structures of M-*m*, HP-*m* (*m*=2, 6, 10) and CP-*x* (*x*=0, 15, 27, 41, 60%)

incorporated M-10 unit in the copolymers determined by <sup>1</sup>H NMR. M-10 and HMA were copolymerized via the conventional free radical polymerization to produce CP10-*x*. A typical polymerization procedure for CP10-41% is presented as follows: M-10 (400 mg, 0.73 mmol), HMA (82.56 mg, 0.49 mmol), AIBN (6.06 mg, 0.037 mmol) and freshly distilled anisole (6 mL) were added into a one-neck round-bottom flask (10 mL) successively

and a clear solution was obtained after stirring. The reaction mixture was bubbled with argon for 20 min in an ice bath and the flask was then sealed and immersed into an oil bath at 70 °C and stirred for 48 h. After being cooled down to the room temperature, the polymerization mixture was added dropwise into methanol (80 mL) under stirring. The precipitate was collected by centrifugation and the obtained solid was washed thoroughly with

**Table 1.** Characterization data of the azo polymers

Entry	Sample <sup>a</sup>	The initial azo monomer content in monomer feed (mol%) <sup>b</sup>	The azo content in polymers (mol %) <sup>c</sup>	Yield (%)	<i>M</i> <sub>n,GPC</sub> <sup>d</sup>	<i>Đ</i> <sup>d</sup>	Thermal transition <i>T</i> (°C) <sup>e</sup>	<i>T</i> <sub>decomp</sub> (°C) <sup>h</sup>	Modulation depth (nm) <sup>i</sup>
1	HP-2	100	100	32	4770	1.15	G 123 <sup>f</sup> G 128 <sup>g</sup>	271	1172
2	HP-6	100	100	34	5000	1.14	G 95 N 133 I <sup>f</sup> I 134 N 100 G <sup>g</sup>	270	1032
3	HP-10	100	100	35	6150	1.17	G 67 S <sub>A</sub> 132 I <sup>f</sup> I 132 S <sub>A</sub> 78 G <sup>g</sup>	269	960
4	CP-60%	80	60	42	8410	1.32	G 53 <sup>f</sup> G 62 <sup>g</sup>	272	945
5	CP-41%	60	41	56	10040	1.61	G 41 <sup>f</sup> G 43 <sup>g</sup>	276	940
6	CP-27%	40	27	64	13290	1.90	G 28 <sup>f</sup> G 30 <sup>g</sup>	282	780
7	CP-15%	20	15	76	15160	1.97	G 10 <sup>f</sup> G 12 <sup>g</sup>	285	500 <sup>j</sup>
8	PHMA	0	0	80	16500	1.84	G -16 <sup>f</sup> G -10 <sup>g</sup>	233	0

<sup>a</sup> HP-*m* (*m*=2, 6, 10) refer to the homopolymer of M-*m*, CP10-*x* (*x*=15%, 27%, 41%, 60%) refer to the copolymers of M-10 and HMA with different azo contents, and PHMA refers to the homopolymer of HMA. <sup>b</sup> The molar percentage of the azo monomer in the initial monomer feed. <sup>c</sup> The molar percentage of the azo unit in the polymers determined by <sup>1</sup>H NMR. <sup>d</sup> The number-average molecular weights (*M*<sub>n,GPC</sub>) and molar-mass dispersities (*Đ*) of the polymers measured by GPC using PS standards. <sup>e</sup> G = glassy; S<sub>A</sub>= Smectic A; N = Nematic; I = isotropic. <sup>f</sup> DSC second heating scan under nitrogen (10 °C/min). <sup>g</sup> DSC first cooling scan under nitrogen (-10 °C/min). <sup>h</sup> The temperatures at 5% weight loss of the samples under nitrogen were measured by TGA heating experiments at a rate of 10 °C/min. <sup>i</sup> The modulation depth of the SRGs was measured by AFM using tapping model. <sup>j</sup> The inscribed SRG on CP-15% film was kept at 0 °C prior to its characterization with AFM.



warm methanol until no monomer was detectable with thin layer chromatography. Finally, the product was dried at 50 °C under vacuum for 48 h to provide the orange copolymer CP10-41% (yield: 56%, entry 5 in Table 1).

The azo copolymers CP10-*x* (*x* = 60%, 27%, 15%) were prepared using the similar process as for CP10-41% (Table 1).

### Preparation of azo polymer films

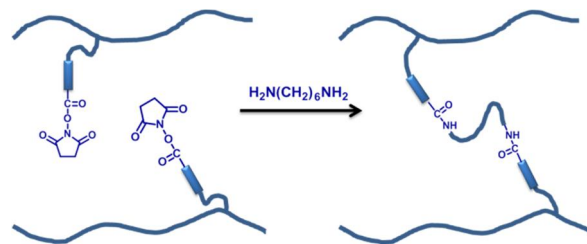
The above-obtained azo polymers were dissolved in dioxane (100 mg/mL) and the resulting solutions were filtered using a 0.45 µm filter. Polymer films were then prepared by spin-coating such polymer solutions onto the pre-cleaned quartz glass plates (which were cleaned in Piranha solution (H<sub>2</sub>SO<sub>4</sub>:H<sub>2</sub>O<sub>2</sub> = 7:3 (v/v)) and rinsed with distilled water) at 2000 rpm for 18 s. The resulting polymer films were annealed at 60 °C in a vacuum oven for 12 h prior to the SRG inscription and their thickness was about 1.1 µm as evaluated by atomic force microscopy (AFM, NT-MDT Instruments, Russia: NTEGRA Prima). The weights of the pure polymer films could be obtained by subtracting the weights of the clean quartz glass plates from the total weights of the quartz glass plates and the supported polymer films.

### Generation of SRGs on the azo polymer films

The experimental setup for SRG formation was similar to that reported before.<sup>70</sup> The SRG inscription was performed by using *p*-polarized green light (532 nm) with an intensity of 180 mW/cm<sup>2</sup>. The angle between two incident coherent laser beams was set at 8° to produce 3.75 µm grating spacing. A set of wave plates and polarizers was used to control the intensities and polarization states of the interfering beams. The SRGs formed on the azo polymer films were monitored by measuring the growth of the first-order diffraction efficiency in the transmission mode with an unpolarized probe He-Ne laser beam at 633 nm of a low intensity (1 mW/cm<sup>2</sup>) in order not to disturb the SRG recording. The diffraction efficiency was obtained through dividing the intensity of the first-order diffraction by the initial incidence intensity of the probe beam. The surface profiles of the resulting gratings were characterized with AFM (NT-MDT Instruments, Russia: NTEGRA Prima) in the tapping mode.

### Chemical crosslinking of the azo polymer films and post-fixation of the SRGs formed on these azo polymer films

The chemical crosslinking of the azo polymer films was carried out by the reaction of *N*-hydroxysuccinimide carboxylate groups on the azo units in the polymers with 1,6-hexanediamine in its methanol solutions (Scheme 2). A series of azo polymer films were immersed into 1,6-hexanediamine solutions in methanol (20 mL) with different concentrations (*C* = 0, 5, 50, 100, 200, 300, and 350 mmol/L) for 20 min and another series were immersed into 1,6-hexanediamine solutions in methanol (20 mL) with a concentration of 350 mmol/L for different times (*t* = 0, 0.5, 1, 2, 4, 8, 12, 16, 20, and 30 min) at 25 °C. The resulting polymer films were washed thoroughly with methanol and then dried under vacuum at 25 °C for 12 h. Afterwards, such polymer films were immersed into 10 mL of THF for 3 h at 25 °C, and the amounts of the azo polymers dissolved in the resulting solutions were evaluated by their UV-vis absorption peak intensities (note that the uncrosslinked azo polymer films could be completely dissolved into THF within 30 s). The residual weights of the fixed



**Scheme 2** Schematic illustration of the crosslinking reaction of *N*-hydroxysuccinimide carboxylate groups on the azo units in the azo polymers with 1,6-hexanediamine.

azo polymer films on the quartz glass plates could be derived by subtracting the above-obtained weights of the dissolved azo polymers from the weights of the original polymer films, from which the residual weight percentages of the fixed azo polymer films on the quartz glass plates could be obtained.

SRGs were inscribed onto the azo polymer films following the above-described process and their surface profiles were characterized with AFM. Two representative polymer (i.e., HP-10 and CP10-41%) films with the SRG patterns were then immersed into a 1,6-hexanediamine solution in methanol (*C* = 350 mmol/L) at 25 °C for different times (*t* = 0, 4, 10, and 15 min). Afterwards, they were taken out and washed thoroughly with methanol and then dried at 25 °C under vacuum for 24 h. The resulting polymer films with fixed SRGs were annealed at temperatures being about 10 °C above the *T<sub>g</sub>* values of the corresponding uncrosslinked azo polymers for different times (*t* = 0.5, 10, 40, 120, 300, 720, and 1440 min) or at 250 °C for 3 h. The unfixed SRGs on CP10-41% films were also annealed for 10, 20, 30, 60, and 90 s at 55 °C, respectively, while the unfixed SRGs on HP-10 films were annealed for 10, 20, 40, 60, 90, 120, and 180 s at 90 °C, respectively. All the remaining modulation depth of the SRGs was recorded by AFM.

### Characterization

<sup>1</sup>H NMR spectra of the samples were recorded on a Mercury Vx-300 spectrometer (300 MHz). The number-average molecular weights (*M<sub>n</sub>*, GPC) and molar-mass dispersities (*Đ*) of the obtained polymers were determined with a gel permeation chromatograph (GPC) equipped with an Agilent 1200 series manual injector, an Agilent 1200 high-performance liquid chromatography (HPLC) pump, an Agilent 1200 refractive index detector, and three Agilent Plgel columns (mixed-C, 104 Å and 500 Å) with 200-3M, 4000-400K, and 500-20K molecular ranges (the temperature of the column oven was 35 °C). THF was used as the eluent at a flow rate of 1 mL/min, and the calibration curve was obtained by using polystyrene (PS) standards. Thermogravimetric analyses (TGA) were performed on a Netzsch TG 209 instrument at a heating rate of 10 °C/min in the nitrogen atmosphere. Differential scanning calorimetry (DSC, Netzsch 204) was utilized to study the thermal transitions of the polymers at a heating/cooling rate of 10 °C/min under nitrogen. The temperature and heat flow scale were calibrated with standard materials including indium (70-190 °C), tin (150-270 °C), zinc (350-450 °C), bismuth (190-310 °C) and mercury (-100-0 °C) in different temperature ranges. The glass transition temperatures (*T<sub>g</sub>*) of the polymers were determined as the midpoints of the step



changes of the heat capacity, while the phase transition temperatures were measured from the maximum/minimum of the endothermic/exothermic peaks. The liquid crystalline textures of the samples were observed by using an Olympus BX51 POM equipped with a Linksys 32 THMSE600 hot stage and a digital camera (micropublisher 5.0 RTV). An UV-vis scanning spectrophotometer (TU 1900, Beijing Purkinje General Instrument Co., Ltd) was utilized to obtain the UV-vis spectra of the samples at 25 °C. X-ray diffraction (XRD) measurements were carried out by using a Bruker D8 FOCUS diffractometer with Cu K $\alpha$  radiation (1.5406 Å) generated at 40 KV and 40 mA from 0.5 to 10° (2 $\theta$  value) at a scanning rate of 1°/min. The SRGs were inscribed onto the azo polymer films by using two coherent laser beams ( $\lambda$  = 532 nm) system (diode-pumped laser, Nd:YVO<sub>4</sub>). The formation of the SRGs was monitored from the change in the first-order diffraction intensity of a He-Ne (633 nm) laser beam on the transmission side using a photodetector. The surface topographies of the azo polymer films were examined using AFM in the tapping mode.

## Results and discussion

### Synthesis and characterization of azo polymers

It is well established that *N*-hydroxysuccinimide carboxylate can easily react with primary amines under mild reaction conditions.<sup>71</sup> Recently, we have synthesized a series of methacrylate type azo monomers with an *N*-hydroxysuccinimide carboxylate substituent and their homopolymers by the free radical polymerization.<sup>68</sup> The obtained azo polymer films proved to be crosslinkable with 1,6-hexanediamine in methanol, but such post-crosslinking process was still relatively slow (about 1 h), probably due to the rigid characteristics of poly(methacrylate) type azo polymers. In addition, the resulting azo polymers had rather high  $T_g$  values ( $\geq 102$  °C as determined by DSC at the second heating processes with a heating rate of 10 °C/min), which might prevent their fast formation of SRGs.<sup>59</sup> To address these issues, we have designed a series of acrylate type azo monomers with an *N*-hydroxysuccinimide carboxylate substituent and subsequently prepared their homo- and copolymers via the free radical polymerization in the present study.

Scheme 1 presents the synthetic route of the acrylate type azo monomers (M-*m* (*m* = 2, 6, 10)) and their polymers. All the intermediates were synthesized following the literature procedure.<sup>67</sup> The desired azo monomers were readily prepared through the coupling reaction between AAzoA-*m* (*m* = 2, 6, 10) and *N*-hydroxysuccinimide, using DCC as the catalyst. Their yields were around 70% and their purities were satisfactory, as determined with both thin layer chromatography and <sup>1</sup>H NMR (Fig. 1a).

The acrylate type azo monomers M-*m* (*m* = 2, 6, 10) were first polymerized via the conventional free radical polymerization at 70 °C using AIBN as the initiator and anisole as the solvent, resulting in their corresponding homopolymers (namely HP-*m* (*m* = 2, 6, 10)). In addition, a series of azo copolymers (namely CP10-*x* (*x* is the molar percentage of the azo unit in the copolymers determined by <sup>1</sup>H NMR)) were also prepared via the free radical copolymerization of M-10 and HMA with different feed ratios. All the azo polymers were purified by their first

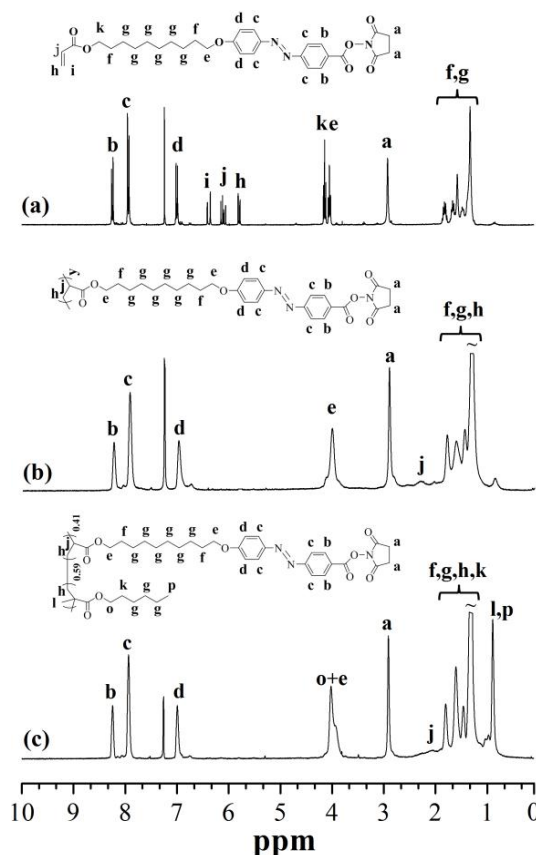


**Fig. 1** <sup>1</sup>H NMR spectra of M-10(a), HP-10 (b) and CP-41% (c) in CDCl<sub>3</sub>.

precipitation into methanol and then washed thoroughly with warm methanol until no monomers could be detected by thin layer chromatography any more. The resulting azo polymers are easily soluble in the common organic solvents such as THF, acetone, and chloroform.

The obtained azo polymers were first characterized with <sup>1</sup>H NMR. Fig. 1b and c shows the <sup>1</sup>H NMR spectra of one representative azo homopolymer HP-10 and one azo copolymer CP10-41%, respectively. It can be seen clearly that the vinyl proton signals of the acrylate group from M-10 have completely disappeared from the spectra of these azo polymers, further demonstrating the absence of the azo monomer in the obtained polymers. Moreover, the chemical shifts and peak integrals of all the protons in the polymers are consistent with their expected structures. Similar results were also obtained for the other polymers. By comparing the integral of the peak a at 2.94 ppm (due to the protons from the succinimide group of the azo unit) and that of the peaks o+e around 4.0 ppm (due to the protons of -CH<sub>2</sub>O- in both the spacer of the azo unit and side chain of HMA unit) in the copolymers, the molar percentages of the M-10 unit incorporated into the azo copolymers could be derived (Table 1). Apparently lower molar percentages of the azo unit were found to be incorporated into the azo copolymers in comparison with those of the azo monomer in the initial monomer feeds, suggesting the higher reactivity of HMA than M-10 in the copolymerization processes.

The molecular weights and molar-mass dispersities (*D*) of the obtained polymers were determined with GPC (Table 1). It can



be seen that the molecular weights of the azo homopolymers increase with increasing the length of their flexible spacers, probably due to the reduced steric hindrance of the azo monomers during the polymerizations with an increase in the spacer length. In comparison, the azo copolymers showed obviously higher molecular weights and they increased with an increase in the contents of the HMA unit in the copolymers, which also could be ascribed to the higher reactivity of HMA than M-10 in the copolymerization processes.

The thermal behaviours of the obtained polymers were analyzed with a combination of TGA, DSC, and POM. The temperatures at 5% weight loss of the azo polymers determined by TGA at a heating rate of 10 °C/min under nitrogen were  $\geq 269$  °C (Table 1), indicating their rather good thermal stability. It is interesting to note that all the azo copolymers exhibit improved thermal stability in comparison with the homopolymers (i.e., PHMA and HP-10), just as reported by Zhang and coworkers.<sup>72</sup> The real reason for this phenomenon is not very clear yet, and further investigation is ongoing to provide a reasonable explanation. The DSC study revealed that HP-6 and HP-10 exhibited one glass transition step and one weak phase transition peak during both the second heating and the first cooling scans (Fig. 2), whereas all the other polymers showed only one glass transition step under the same conditions. A glass transition temperature ( $T_g$ ) of -10, 12, 30, 43, 62, 78, 100 and 128 °C was observed in the DSC second heating scan for PHMA, CP10-15%, CP10-27%, CP10-41%, CP10-60%, HP-10, HP-6 and HP-2, respectively, indicating that the  $T_g$  values of the azo copolymers increased with an increase in their azo contents and those of the azo homopolymers decreased with an increase in the spacer length, just as previously reported.<sup>69,73</sup>

The POM study revealed that only HP-6 and HP-10 showed

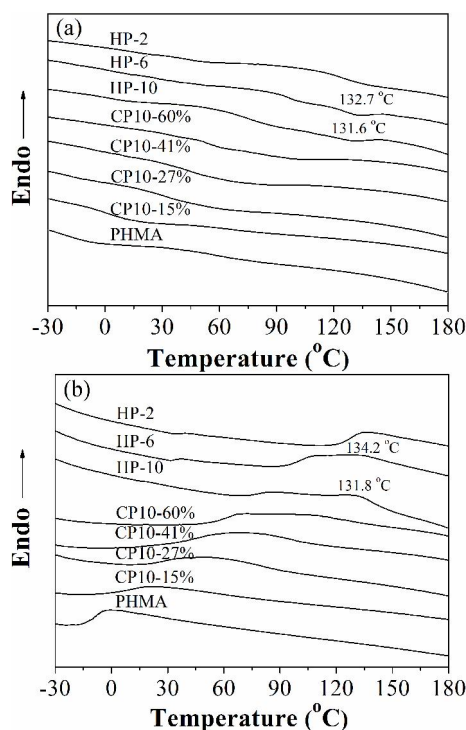


**Fig. 2** DSC curves of the polymers from the first cooling scan (a) and from the second heating scan (b) ( $\pm 10$  °C/min).

obvious liquid crystalline textures (Fig. S1). Their birefringences disappeared completely at 137 and 135 °C upon heating (10 °C/min), respectively, and they appeared again at 131 and 130 °C upon cooling from the isotropic states at a rate of 10 °C/min, respectively, which indicated that the phase transition peaks in their DSC curves represented the transition between liquid crystalline and isotropic phases. XRD studies demonstrated that HP-6 had a nematic liquid crystalline mesophase, whereas a smectic A liquid crystalline phase was present in HP-10 (Fig. S2). In contrast to HP-6 and HP-10, no liquid crystalline phases were observed for the azo copolymers and HP-2, probably due to the disruption of the ordered structures by the incorporation of HMA unit into the copolymers and the too short spacer length in HP-2.

### Crosslinkability of the azo polymer films

The crosslinking of the azo homopolymer (HP- $m$  ( $m = 2, 6, 10$ )) and copolymer (CP10- $x$  ( $x = 15, 27, 41, 60\%$ )) films was investigated to shed light on the influences of the polymer structures on their crosslinking processes. The azo polymer films with almost same thickness ( $\sim 1.1$   $\mu\text{m}$ ) were first prepared via spin-coating on the clean quartz glass plates, which were subsequently annealed at 60 °C in a vacuum oven for 12 h prior to their further studies, leading to the transparent films in an amorphous state (as revealed by POM). It is also worth mentioning here that such azo polymer films could undergo reversible photochemical isomerisation upon the alternating UV and visible light irradiations (Fig. S3).

The above-obtained azo polymer films were then immersed into a series of 1,6-hexanediamine solutions in methanol with different concentrations for a fixed crosslinking time or immersed into a 1,6-hexanediamine solution in methanol with a fixed concentration but for different crosslinking times. The resulting polymer films were then immersed into 10 mL of THF for 3 h. The uncrosslinked azo polymer films were found to be completely dissolved in THF within 30 s, whereas the other azo polymer films crosslinked under different conditions showed improved resistance to THF to different extents. The dissolved weight percentages of the polymer films could be obtained through characterizing the resulting solutions by measuring their UV-vis absorptions, from which the residual weight percentages of the remaining films on the quartz glass plates could be derived (which can be used to represent the crosslinking degrees of the azo polymer films) (Fig. 3a and b). Fig. 3a shows that the residual weight percentages of the azo polymer films (or their crosslinking degrees) increase with an increase in the crosslinker concentrations for a fixed crosslinking time, just as expected. In addition, the chemical structures of the azo polymers also showed an obvious influence on their crosslinking processes. While a crosslinker concentration of 300 mmol/L was required for HP-2, HP-6, HP-10 and CP10-60% to achieve their maximum crosslinking in 20 min, complete crosslinking was achieved for CP10-41%, CP10-27% and CP10-15% with a crosslinker concentration of 100 mmol/L in the same time period (Fig. 3a), which demonstrated that the crosslinking rates of the azo polymer films increased with increasing the incorporated HMA contents in the azo polymers. Fig. 3b shows that the crosslinking degrees of the azo polymer films increase with an increase in the crosslinking times at a fixed crosslinker concentration, but they decrease with increasing the azo contents in the copolymers. It



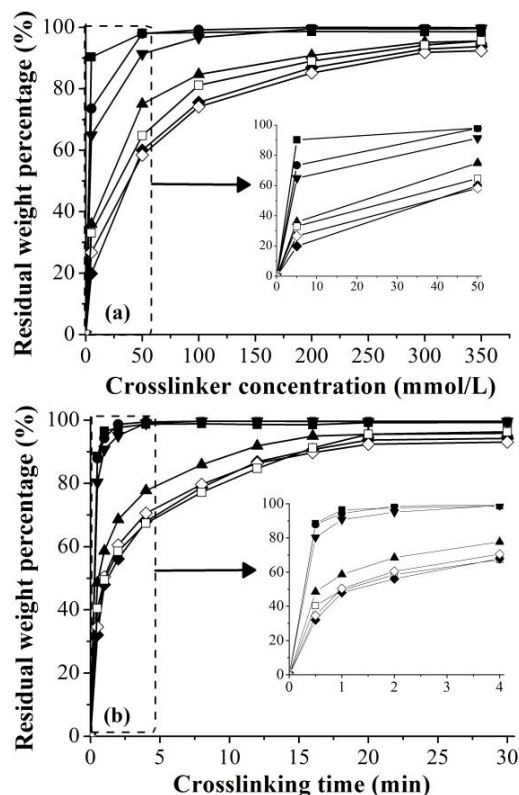


**Fig. 3** Dependence of the residual weight percentages of the crosslinked azo polymer films (after their immersion in THF for 3 h) on the concentrations of the 1,6-hexanediamine solution in methanol with a fixed crosslinking time of 20 min (a) or on the crosslinking time with a fixed 1,6-hexanediamine concentration in methanol (350 mmol/L) (b) (HP-2 (□), HP-6 (◇), HP-10 (◆), CP-60% (▲), CP-41% (▼), CP-27% (●), CP-15% (■)).

requires 20 min for HP-2, HP-6, HP-10 and CP10-60% to achieve the maximum crosslinking, whereas 4 min is enough for fully crosslinking CP10-15%, CP10-27% and CP10-41%. The faster crosslinking rates of the azo copolymers with a higher incorporated HMA content (i.e., CP10-15%, CP10-27%, and CP10-41%) in comparison with the azo homopolymers (HP-*m* (*m* = 2, 6, 10)) and azo copolymer with a lower HMA content (i.e., CP10-60%) might be attributed to the higher swelling ability of the former azo polymers in the solutions (Fig. S6 and S7). Note that the optical transparency of most of the azo polymer films was not much affected by the crosslinking processes (Fig. S8), which is important for their practical applications.

Fig. 4 presents the FT-IR spectra of the uncrosslinked and crosslinked HP-10 films. It can be seen clearly that in comparison with the FT-IR spectrum of the uncrosslinked azo polymer film, several new absorption peaks around 1535  $\text{cm}^{-1}$  (amide II band, N-H deformation vibration), 1670  $\text{cm}^{-1}$  (amide I band, C=O stretching), and 3326  $\text{cm}^{-1}$  (N-H stretching) were observed in that of the crosslinked polymer film. This, together with the disappearance of the peak around 1770  $\text{cm}^{-1}$  (the imide band of the succinimide group from the uncrosslinked polymer) in the FT-IR spectrum of the crosslinked HP-10 film, provided strong and direct evidence for the occurrence of the chemical crosslinking reaction between the hydroxysuccinimide groups on the polymer chains and 1,6-hexanediamine (Scheme 2).

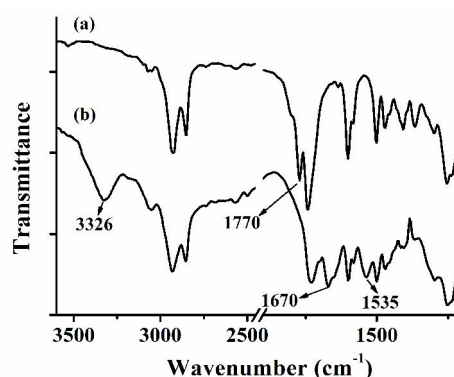


**Fig. 4** FT-IR spectra of the uncrosslinked (a) and crosslinked (b) HP-10 films (the crosslinked HP-10 film was obtained by immersing its uncrosslinked one into a 1,6-hexanediamine solution in methanol (350 mmol/L) for 15 min. Another uncrosslinked HP-10 film and this crosslinked one were then peeled off from the quartz glass plates by immersing them into methanol and sonicating for 1 min, dried, and then ground with KBr powder for FT-IR measurements).

On the basis of the above results, we can conclude that the obtained side-chain azo polymers containing *N*-hydroxysuccinimide carboxylate-substituted azo groups could be easily crosslinked with 1,6-hexanediamine under mild conditions, which is highly promising for the post-fixation of the SRGs formed on such polymer films.

#### The photoinduced diffraction efficiency and SRGs on the azo polymer films

An Nd:YVO<sub>4</sub> laser was applied to inscribe SRGs on the azo polymer films by using the interference pattern. Special care was taken to prepare amorphous azo polymer films with almost same thickness in order to exclude both the effect of confinement<sup>56</sup> and the influence of the liquid crystalline phases on the formation of SRGs.<sup>74</sup> The SRG formation processes were probed by monitoring the diffraction of the films with a low intensity He-Ne laser beam (633 nm, 1  $\text{mw}/\text{cm}^2$ ). The diffraction efficiency was obtained through dividing the intensity of the first-order diffraction by the initial incidence intensity of the probe beam. Fig. 5 shows the changes in the first-order diffraction efficiency

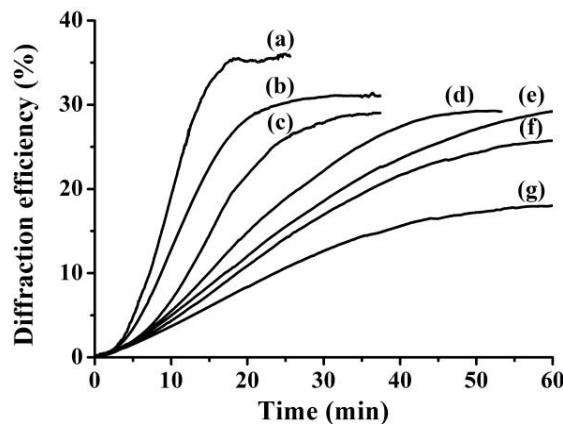


**Fig. 5** Time dependence of the first-order diffraction efficiency for the films of HP-2 (a), HP-6 (b), HP-10 (c), CP10-60% (d), CP10-41% (e), CP10-27% (f), and CP10-15% (g).



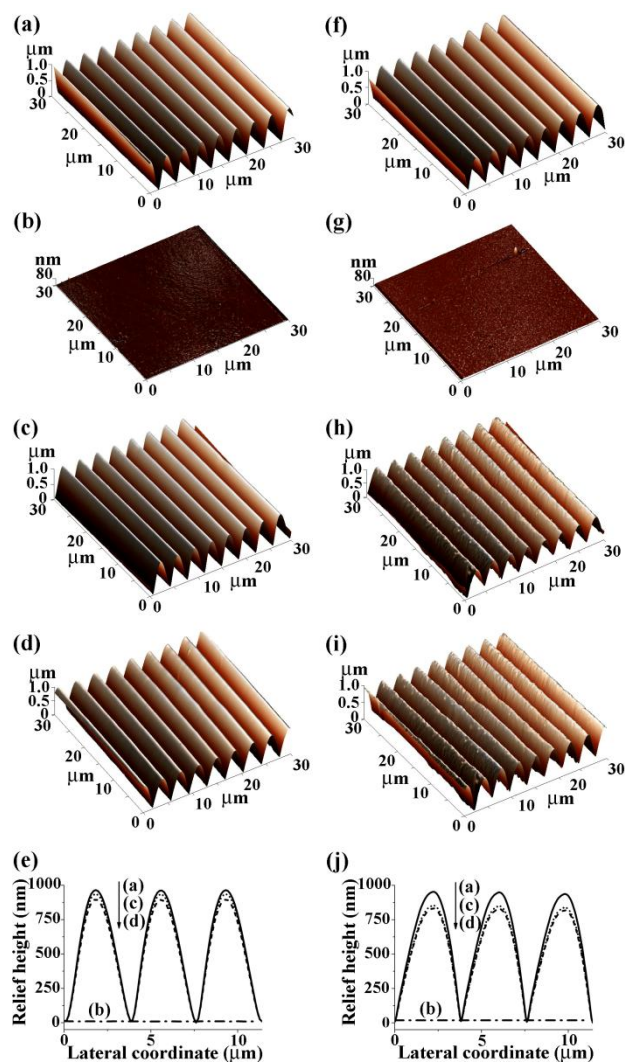


**Fig. 6** Topographical AFM images of the SRGs formed on HP-10 (a-d) and CP10-41% (f-i) films: (a,f) Uncrosslinked HP-10 (a) and CP10-41% (f) films without annealing; (b,g) Uncrosslinked polymer films annealed for 3 min (HP-10 film at 90 °C (b) and CP10-41% film at 55 °C (g)); (c,h) Crosslinked HP-10 film (crosslinked in a 1,6-hexanediamine solution (350 mmol/L) for 15 min) annealed at 90 °C for 24 h (c) and crosslinked CP10-41% film (crosslinked in a 1,6-hexanediamine solution (350 mmol/L) for 4 min) annealed at 55 °C for 24 h (h); (d,i) HP-10 (d) and CP10-41% (i) films were crosslinked with the same conditions as in (c,h) and then immersed into THF for 24 h; (e,j) AFM cross-sectional profiles taken from the samples a-d (e) and those taken from the samples f-i (j).

as a function of the laser irradiation time for the azo polymer films. It can be seen clearly that the diffraction efficiency values of the azo polymer films can reach a plateau within 18-60 min. Both the inscription rates and diffraction efficiency saturation values of the azo homopolymer films were found to increase with a decrease in their flexible spacer length, while those of the azo copolymer films proved to essentially increase with an increase in the azo contents in the copolymers.<sup>56, 75, 76</sup> The above results clearly demonstrated that an increase in the azo contents in the azo polymers had an obvious positive effect on the formation of

SRGs on their films. In addition, they also suggested that the mass migration of the azo polymer films was driven by the azo chromophores and the longer spacer might dissipate more driven energy obtained from the light irradiation.<sup>53</sup> The mechanism of the current observations could be partially elucidated by using the optical-field gradient force model proposed by Kumar et al.<sup>49, 77</sup> The formation of SRGs on the azo polymer films was confirmed by AFM (Fig. 6a and f). The grating profiles exhibited a sinusoidal shape and their periods agreed well with the designed value (i.e., 3.75  $\mu\text{m}$ ). The modulation depth of the SRGs formed on the azo polymer films was more than 500 nm in all cases (Tables 1 and S2), demonstrating the high efficiency of our azo polymers in the formation of SRGs. In addition, the order of their depth was almost the same as that of their corresponding diffraction efficiency values.

#### 40 Post-fixation of SRGs

It is known that the SRGs formed on the amorphous azo polymer films are only stable at temperatures below their  $T_g$  and can be easily erased by heating above their  $T_g$ . This was also confirmed to be true for our azo polymer systems. The photoinduced SRGs on our uncrosslinked azo polymer films proved to be stable as long as they were kept at temperatures below their  $T_g$ . However, these inscribed SRGs were completely disappeared quickly after their annealing at temperatures being about 10 °C above their  $T_g$  (Fig. 6b and g, Fig. 7). In addition, such uncrosslinked azo polymer films with inscribed SRGs could be quickly dissolved when they were immersed into common organic solvents (e.g., THF) (Figures not shown). These results clearly demonstrated that the photoinduced SRGs on the uncrosslinked azo polymer films are not resistant to higher temperatures and organic solvents, which may have negative influence on their future applications.

We then tried to improve the shape stability of the SRGs formed on the azo polymer films by crosslinking them in the 1,6-hexanediamine solutions in methanol. It can be seen clearly that the post-fixation of SRGs on the azo polymer films by their

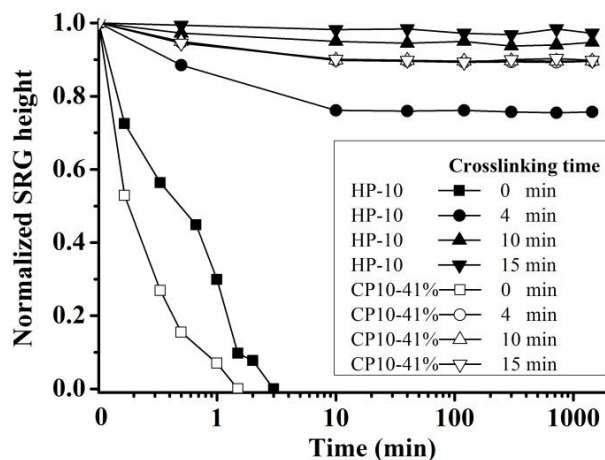


**Fig. 7** Dependence of the normalized SRG heights for the uncrosslinked and crosslinked HP-10 films (filled symbols, annealing temperature: 90 °C) and CP10-41% films (empty symbols, annealing temperature: 55 °C) on the annealing times (the azo polymer films were crosslinked in a 1,6-hexanediamine solution in methanol (350 mmol/L) for 0, 4, 10, and 15 min, respectively).



crosslinking significantly enhanced their stability at higher temperatures, even for a rather short crosslinking time of 4 min (Fig. 7). While the surface SRG structures on the uncrosslinked azo polymer films could be completely erased within 3 min for HP-10 film at 90 °C and within 1.5 min for CP10-41% film at 55 °C, respectively (Fig. 6b and g, Fig. 7), those on the crosslinked polymer films (with a crosslinking time  $\geq 4$  min for CP10-41% film and  $\geq 10$  min for HP-10 film) remained almost intact after 24 h of annealing at temperatures being about 10 °C above their corresponding  $T_g$  (Fig. 6c and h, Fig. 7). In addition, the SRGs on the crosslinked polymer films were also well preserved even after their immersing in THF (a good solvent for the uncrosslinked azo polymer films) for 24 h (Fig. 6d and i). Fig. 6e and j shows the cross-sectional profiles taken from the corresponding samples before and after heating or rinsing with THF, which demonstrated the stability of the SRGs on the crosslinked azo polymer films more clearly. Furthermore, the SRGs on the crosslinked azo polymer (HP-10 and CP10-41%) films could be retained without obvious damage even at a high annealing temperature of 250 °C for 3 h (Fig. 8), which strongly demonstrated the high efficiency of our post-fixation strategy. In this context, it is worth mentioning that the post-crosslinking of the azo polymer films with SRGs hardly affected their diffraction efficiencies, indicating the negligible influence of the post-crosslinking treatment on their optical properties (Fig. S9).

## Conclusions

We have demonstrated for the first time a facile and highly efficient approach to achieve fast and stable fixation of the photoinduced surface relief gratings on the azo polymer films by the design and synthesis of a series of new easily crosslinkable azo homopolymers and copolymers with *N*-hydroxysuccinimide carboxylate-substituted azo moieties and relatively low glass transition temperatures via the conventional free radical

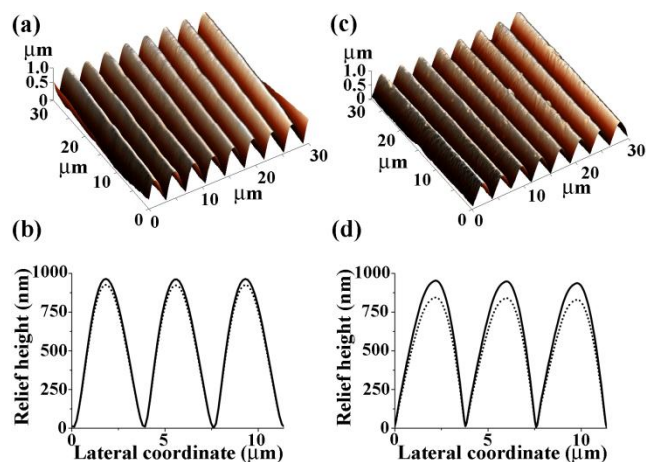


**Fig. 8** (a,c) Topographical AFM images of SRGs on the crosslinked HP-10 (a) and CP10-41% (c) films after their annealing at 250 °C for 3 h (the polymer films were crosslinked in a 1,6-hexanediamine solution in methanol (350 mmol/L) for 15 min for HP-10 and 4 min for CP10-41%, respectively); (b,d) AFM cross-sectional profiles taken from the crosslinked HP-10 film (b) and CP10-41% film (d) before (solid line) and after their annealing (short dot) at 250 °C for 3 h.

The chemical structures of the azo polymers showed much influence on the crosslinking ability of their films as well as the photoinduced diffraction efficiency and surface relief gratings on their films. All the obtained azo polymer films proved easily crosslinkable within 4-15 min with 1,6-hexanediamine in methanol under mild conditions, and faster crosslinking was observed for the azo copolymers in comparison with the azo homopolymers. In particular, the resulting fixed surface relief gratings could be kept almost intact at temperatures being about 10 °C above the glass transition temperatures of the uncrosslinked azo polymers for 24 h or at 250 °C for 3 h or even after their immersion into a good solvent of the uncrosslinked azo polymers for 24 h. In view of the easy synthesis of such easily crosslinkable azo polymers that can have a high azo content up to 100%, their very fast post-crosslinking under mild conditions, the high resistance of the fixed surface relief gratings towards both high temperatures and organic solvents, and the negligible influence of the post-fixation treatment on the optical transparency of the azo polymer films, we believe that such azo polymers are highly promising for surface relief grating applications as well as for many other areas such as photoresponsive liquid crystalline elastomers.

## Acknowledgments

The authors gratefully acknowledge the financial support from National Natural Science Foundation of China (20974048, 51103075), Natural Science Foundation of Tianjin (10JCYBJC02100, 11JCYBJC01500, 14JCQNJC03800), and PCSIRT (IRT1257).

## Notes and references

- <sup>a</sup> Key Laboratory of Functional Polymer Materials, Ministry of Education, State Key Laboratory of Medicinal Chemical Biology, Collaborative Innovation Center of Chemical Science and Engineering (Tianjin), and College of Chemistry, Nankai University, Tianjin 300071, P. R. China. E-mail: zhanghuiqi@nankai.edu.cn
- <sup>b</sup> MOE Key Laboratory of Weak Light Nonlinear Photonics, Tianjin Key Laboratory of Photonics and Technology of Information Science, School of Physics, Nankai University, Tianjin 300071, P. R. China.
- <sup>†</sup> Electronic Supplementary Information (ESI) available: Supplementary data, including (1) POM images of azo polymers upon cooling; (2) XRD characterization of the azo polymers; (3) photochemical behaviours of the azo polymer films; (4) swelling ability of the azo polymer films in methanol; (5) effect of crosslinking on the optical transparency of the azo polymer films; (6) effect of crosslinking on the diffraction efficiency of the azo polymer films with inscribed SRG structures. See DOI: 10.1039/b000000x/
- 1 M. Dumont, G. Froc and S. Hosotte, *Nonlinear Opt.*, 1995, **9**, 327-338.
- 2 J. Kato, I. Yamaguchi and H. Tanaka, *Opt. Lett.*, 1996, **21**, 767-769.
- 3 Y. Wang, G. Ye and X. Wang, *J. Mater. Chem.*, 2012, **22**, 7614-7621.
- 4 M. Ivanov, D. Ilieva, G. Minchev, T. Petrova, V. Dragostinova, T. Todorov and L. Nikolova, *Appl. Phys. Lett.*, 2005, **86**, 181902.
- 5 C.-U. Bang, A. Shishido and T. Ikeda, *Macromol. Rapid Commun.*, 2007, **28**, 1040-1044.
- 6 M. Natali and S. Giordani, *Chem. Soc. Rev.*, 2012, **41**, 4010-4029.
- 7 G. Shen, G. Xue, J. Cai, G. Zou, Y. Li, M. Zhong and Q. Zhang, *Soft Matter*, 2012, **8**, 9127-9131.
- 8 Y. L. Yu, M. Nakano and T. Ikeda, *Nature*, 2003, **425**, 145-145.



- 9 T. J. White, N. V. Tabiryan, S. V. Serak, U. A. Hrozhyk, V. P. Tondiglia, H. Koerner, R. A. Vaia and T. J. Bunning, *Soft Matter*, 2008, **4**, 1796-1798.
- 10 C. L. van Oosten, C. W. M. Bastiaansen and D. J. Broer, *Nat. Mater.*, 2009, **8**, 677-682.
- 11 W. Wang, X. Sun, W. Wu, H. Peng and Y. Yu, *Angew. Chem. Int. Ed.*, 2012, **51**, 4644-4647.
- 12 L. Fang, H. Zhang, Z. Li, Y. Zhang, Y. Zhang and H. Zhang, *Macromolecules*, 2013, **46**, 7650-7660.
- 13 H. Yang, G. Ye, X. Wang and P. Keller, *Soft Matter*, 2011, **7**, 815-823.
- 14 Y. Zhao, S. Bai, D. Dumont and T. V. Galstian, *Adv. Mater.*, 2002, **14**, 512-514.
- 15 H. Wen, W. Zhang, Y. Weng and Z. Hu, *RSC Advances*, 2014, **4**, 11776-11781.
- 16 D. Y. Kim, S. K. Tripathy, L. Li and J. Kumar, *Appl. Phys. Lett.*, 1995, **66**, 1166-1168.
- 17 P. Rochon, E. Batalla and A. Natansohn, *Appl. Phys. Lett.*, 1995, **66**, 136-138.
- 18 Y. Zhao, T. Ikeda Smart, light-responsive materials: Azobenzene-containing polymers and liquid crystals. *John Wiley & Sons*; 2009.
- 19 H. Yu, K. Okano, A. Shishido, T. Ikeda, K. Kamata, M. Komura, T. Iyoda, *Adv. Mater.* 2005, **17**, 2184-2188.
- 20 M. Ishiguro, D. Sato, A. Shishido and T. Ikeda, *Langmuir*, 2006, **23**, 332-338.
- 21 H. Yu, Y. Naka, A. Shishido, T. Ikeda, *Macromolecules* 2008, **41**, 7959-7966.
- 22 K. Nishizawa, S. Nagano and T. Seki, *Chem. Mater.*, 2009, **21**, 2624-2631.
- 23 X. Xue, J. Zhu, Z. Zhang, N. Zhou, Y. Tu and X. Zhu, *Macromolecules*, 2010, **43**, 2704-2712.
- 24 D. Wang, G. Ye, X. Wang and X. Wang, *Adv. Mater.*, 2011, **23**, 1122-1125.
- 25 L. M. Goldenberg, V. Lisinetskii, Y. Gritsai, J. Stumpe and S. Schrader, *Adv. Mater.*, 2012, **24**, 3339-3343.
- 26 R. Ahmed, A. Priimagi, C. F. J. Faul and I. Manners, *Adv. Mater.*, 2012, **24**, 926-931.
- 27 N. S. Yadavalli, F. Linde, A. Kopyshv and S. Santer, *ACS Appl. Mater. Interfaces*, 2013, **5**, 7743-7747.
- 28 L. M. Goldenberg, Y. Gritsai, O. Kulikovska and J. Stumpe, *Opt. Lett.*, 2008, **33**, 1309-1311.
- 29 J. M. Schumers, C. A. Fustin, J. F. Gohy, *Macromol. Rapid Commun.*, 2010, **31**, 1588-1607.
- 30 F. You, M. Y. Paik, M. Häckel, L. Kador, D. Kropp, H. W. Schmidt and C. K. Ober, *Adv. Funct. Mater.*, 2006, **16**, 1577-1581.
- 31 K. Harada, M. Itoh, T. Yatagai and S.-i. Kamemaru, *Opt. Rev.*, 2005, **12**, 130-134.
- 32 A. S. Matharu, S. Jeeva and P. S. Ramanujam, *Chem. Soc. Rev.*, 2007, **36**, 1868-1880.
- 33 T. Ubukata, M. Hara, K. Ichimura and T. Seki, *Adv. Mater.*, 2004, **16**, 220-223.
- 34 Y. Gritsai, L. M. Goldenberg, O. Kulikovska and J. Stumpe, *J. Opt. A: Pure Appl. Opt.*, 2008, **10**, 125304.
- 35 A. Kravchenko, A. Shevchenko, V. Ovchinnikov, A. Priimagi and M. Kaivola, *Adv. Mater.*, 2011, **23**, 4174-4177.
- 36 D. Xia, Z. Ku, S. C. Lee and S. R. J. Brueck, *Adv. Mater.*, 2011, **23**, 147-179.
- 37 S. Lee, H. S. Kang and J.-K. Park, *Adv. Mater.*, 2012, **24**, 2069-2103.
- 38 S. Wu and J. Huang, *RSC Advances*, 2012, **2**, 12084-12087.
- 39 G. Ye, C. Yang and X. Wang, *Macromol. Rapid. Commun.*, 2010, **31**, 1332-1336.
- 40 Y. Fuchs, O. Soppera, A. G. Mayes and K. Haupt, *Adv. Mater.*, 2013, **25**, 566-570.
- 41 M.-J. Kim, J. Lee, C. Chun, D.-Y. Kim, S. Higuchi and T. Nakayama, *Macromol. Chem. Phys.*, 2007, **208**, 1753-1763.
- 42 L. M. Goldenberg, Y. Gritsai and J. Stumpe, *J. Opt.*, 2011, **13**, 075601.
- 43 X. Wang, J. Yin and X. Wang, *Polymer*, 2011, **52**, 3344-3356.
- 44 J. E. Koskela, J. Vapaavuori, J. Hautala, A. Priimagi, C. F. J. Faul, M. Kaivola and R. H. A. Ras, *J. Phys. Chem. C*, 2012, **116**, 2363-2370.
- 45 X. L. Jiang, L. Li, J. Kumar, D. Y. Kim and S. K. Tripathy, *Appl. Phys. Lett.*, 1998, **72**, 2502-2504.
- 46 J. A. Delaire and K. Nakatani, *Chem. Rev.*, 2000, **100**, 1817-1846.
- 47 A. Natansohn and P. Rochon, *Chem. Rev.*, 2002, **102**, 4139-4176.
- 48 C. J. Barrett, A. L. Natansohn and P. L. Rochon, *J. Phys. Chem.*, 1996, **100**, 8836-8842.
- 49 J. Kumar, L. Li, X. L. Jiang, D.-Y. Kim, T. S. Lee and S. Tripathy, *Appl. Phys. Lett.*, 1998, **72**, 2096-2098.
- 50 P. Lefin, C. Fiorini and J.-M. Nunzi, *Pure Appl. Opt.*, 1998, **7**, 71-82.
- 51 T. G. Pedersen, P. M. Johansen, N. C. R. Holme, P. S. Ramanujam and S. Hvilsted, *Phys. Rev. Lett.*, 1998, **80**, 89-92.
- 52 K. G. Yager and C. J. Barrett, *Macromolecules*, 2006, **39**, 9320-9326.
- 53 D. Wang, G. Ye, Y. Zhu and X. Wang, *Macromolecules*, 2009, **42**, 2651-2657.
- 54 T. S. Lee, D.-Y. Kim, X. L. Jiang, L. Li, J. Kumar and S. Tripathy, *J. Polym. Sci. Part A Polym. Chem.*, 1998, **36**, 283-289.
- 55 J. P. Chen, F. L. Labarthe, A. Natansohn and P. Rochon, *Macromolecules*, 1999, **32**, 8572-8579.
- 56 T. Fukuda, H. Matsuda, T. Shiraga, T. Kimura, M. Kato, N. K. Viswanathan, J. Kumar and S. K. Tripathy, *Macromolecules*, 2000, **33**, 4220-4225.
- 57 Y. Wu, A. Natansohn and P. Rochon, *Macromolecules*, 2001, **34**, 7822-7828.
- 58 L. Andruzzi, A. Altomare, F. Ciardelli, R. Solaro, S. Hvilsted, P. S. Ramanujam, *Macromolecules*, 1999, **32**, 448-54.
- 59 N. Zettsu, T. Ubukata, T. Seki and K. Ichimura, *Adv. Mater.*, 2001, **13**, 1693-1697.
- 60 N. Zettsu and T. Seki, *Macromolecules*, 2004, **37**, 8692-8698.
- 61 W. Li, S. Nagano and T. Seki, *New J. Chem.*, 2009, **33**, 1343-1348.
- 62 H. Takase, A. Natansohn and P. Rochon, *Polymer*, 2003, **44**, 7345-7351.
- 63 T. Kimura, J. Y. Kim, T. Fukuda and H. Matsuda, *Macromol. Chem. Phys.*, 2002, **203**, 2344-2350.
- 64 J. Vapaavuori, V. Valtavirta, T. Alasaarela, J. I. Mamiya, A. Priimagi, A. Shishido and M. Kaivola, *J. Mater. Chem.*, 2011, **21**, 15437-15441.
- 65 N. Zettsu, T. Ogasawara, N. Mizoshita, S. Nagano and T. Seki, *Adv. Mater.*, 2008, **20**, 516-521.
- 66 L. M. Goldenberg, L. Kulikovska, O. Kulikovska and J. Stumpe, *J. Mater. Chem.*, 2009, **19**, 8068-8071.
- 67 H. Q. Zhang, W. Q. Huang, C. X. Li and B. L. He, *Acta. Polym. Sin.*, 1999, 48-54.
- 68 X. Li, R. Wen, Y. Zhang, L. Zhu, B. Zhang and H. Zhang, *J. Mater. Chem.*, 2009, **19**, 236-245.



- 69 X. Li, L. Fang, L. Hou, L. Zhu, Y. Zhang, B. Zhang and H. Zhang, *Soft Matter*, 2012, **8**, 5532-5542.
- 70 H. Nakano, T. Tanino and Y. Shirota, *Appl. Phys. Lett.*, 2005, **87**, 061910.
- 5 71 L. García-Uriostegui, G. Burillo and E. Bucio, *Eur. Polym. J.*, 2010, **46**, 1074-1083.
- 72 H. Yang, J. Xu, S. Pispas and G. Zhang, *Macromolecules*, 2012, **45**, 3312-3317.
- 73 H. Q. Zhang, W. Q. Huang, C. X. Li and B. L. He, *Eur. Polym. J.*,  
10 1998, **34**, 1521-1529.
- 74 N. Zettsu, T. Ogasawara, R. Arakawa, S. Nagano, T. Ubukata and T. Seki, *Macromolecules*, 2007, **40**, 4607-4613.
- 75 J. Vapaavuori, A. Priimagi and M. Kaivola, *J. Mater. Chem.*, 2010, **20**, 5260-5264.
- 15 76 V. Börger, O. Kuliskovska, K. G.-Hubmann, J. Stumpe, M. Huber and H. Menzel, *Macromol. Chem. Phys.*, 2005, **206**, 1488-1496.
- 77 S. Bian, J. M. Williams, D. Y. Kim, L. Li, S. Balasubramanian, J. Kumar and S. Tripathy, *J. Appl. Phys.*, 1999, **86**, 4498-4508.